https://doi.org/10.5194/egusphere-2026-4293
Preprint. Discussion started: 30 July 2026

Development and first application of a new online system for continuous measurement of oxidative potential

Thomas Audoux[1,2], Ambre Delater[3], Manuella Ghanem[2], Jean-Baptiste Lily[2], Mathieu Cazaunau[3], Edouard Pangui[3], Bénédicte Picquet-Varrault[4], Patrice Coll[3], Esperanza Perdrix[1], Laurent Y. Alleman[1], Davy Rousset[2]*

[1]Center for Energy and Environment, IMT Nord Europe, Institut Mines-Télécom, Université de Lille, Lille, France
[2]Department of Pollutant Metrology, Institut National de Recherche et de Sécurité (INRS), 54500 Vandœuvre-lès-Nancy, France
[3]Université Paris Cité and Univ Paris Est Creteil, CNRS, LISA, F-75013 Paris, France
[4]Univ Paris Est Creteil and Université Paris Cité, CNRS, LISA, F-94010 Créteil, France

Correspondence to: Davy Rousset (davy.rousset@inrs.fr)

Abstract. This study introduces a new online system for measuring oxidative potential (OP), using the dithiothreitol (DTT) assay with a direct-to-reagent approach. The instrument enables real-time OP^{DTT} assessments with 5-minute resolution and a competitive instrumental detection limit (0.066 $nmol_{DTT}$ min^{-1}). Its performance was evaluated using model compounds and under controlled experiments in the CESAM atmospheric simulation chamber. The system exhibited clear and consistent responses to major OP-active species, including quinones, copper, manganese, secondary organic aerosols (SOA), and black carbon. In chamber experiments conducted without photochemistry, the OP_v^{DTT} values remained consistently lower than during experiments involving photochemistry, despite the higher concentrations of metals and similar particulate masses. This finding underscores the critical role of photochemically produced species in driving OP. Overall, the instrument demonstrated its capacity to monitor OP_v^{DTT} at a high temporal resolution, paving the way for a deeper understanding of the influences on OP from emission sources and atmospheric processes, particularly transient ones.

1 Introduction

Exposure to atmospheric particulate matter (PM) has been associated with several acute and chronic adverse health effects, such as cardiovascular and respiratory morbidity (Gauderman et al., 2000), asthma (Li et al., 2023), an increased risk of depression and anxiety (Yang et al., 2023) and premature mortality (Lelieveld et al., 2015). It is now recognized that the health impacts of PM are influenced not only by its mass but also by its physical characteristics, chemical composition, and reactivity (Harrison and Yin, 2000; Kelly and Fussell, 2012). Consequently, identifying a toxicity-based metric that integrates these various parameters is essential for a more comprehensive assessment of PM health effects. Oxidative stress is a key initial step in the biological pathway by which PM leads to various adverse health effects (Nel et al., 2006). The presence of reactive oxygen species (ROS) in inhaled air may cause oxidative stress (Delfino et al., 2013; Kelly, 2003; Nel et al., 2006).
The oxidative potential (OP) of PM is defined as its capacity to oxidize target molecules (European Parliament, 2024). In other words, OP is the ability of PM to induce depletion of antioxidants or chemical substitutes, either directly through ROS carried

https://doi.org/10.5194/egusphere-2026-4293
Preprint. Discussion started: 30 July 2026

to the air-lung interface by PM (PM-bound ROS) or by the gas phase, or indirectly through ROS produced endogenously through catalytic reactions between inhaled PM (*e.g.*, transition metals) and the biological system (Dellinger et al., 2001; Knaapen et al., 2004; Lakey et al., 2016). The OP takes into account relevant properties of aerosol particles, including the size, surface area, solubility, and chemical composition of PM, and combines them into a single toxicity indicator (He and Zhang, 2023; Kelly and Fussell, 2012). Thus, OP could provide additional information that particle mass concentration alone may not fully capture. It could also facilitate the implementation of particulate control measures targeting more specifically their toxicity, which is a more effective mitigation strategy for preventing PM-related health impacts (Tassel et al., 2025).

Numerous acellular assays have been developed to measure OP, offering higher reproducibility and accuracy, as well as lower material costs, time, and effort in comparison with cellular assays (Bates et al., 2019). Common acellular assays include the use of 1,4-dithiothreitol (OP^{DTT}), ascorbic acid (OP^{AA}), glutathione (OP^{GSH}), and 2',7'-dichlorodihydrofluorescein (ROS^{DCFH}) (Calas et al., 2018; Shahpoury et al., 2022). Among them, the DTT assay has emerged as the preeminent method for measuring aerosol OP and has been widely adopted (Bates et al., 2019). Its molecular structure features a disulfide bond, similar to that of glutathione, a key antioxidant found in lung lining fluid, conferring it physiological relevance. The OP^{DTT} method monitors the depletion of the reduced form of DTT in the presence of PM due to its oxidation to the disulfide form. This reaction is triggered by the ability of PM to catalyze the transfer of electrons from DTT to oxygen. DTT has been shown to act as a surrogate for the cellular oxidant NADPH (Nicotinamide adenine dinucleotide phosphate), which reduces oxygen to the superoxide anion (O_2^-) (Cho et al., 2005; Hellack et al., 2017). Studies have demonstrated a strong correlation between DTT assays and various biological markers of adverse health effects induced by PM exposure, including airway and nasal inflammation, diabetes, and ischemic heart disease (Abrams et al., 2017; Bates et al., 2015; Delfino et al., 2013; Janssen et al., 2015; Strak et al., 2017; Yang et al., 2016). Measurement of OP is explicitly mentioned in the new directive on air quality in Europe (European Parliament, 2024) and OP^{DTT} has already undergone international interlaboratory comparison within the framework of RI URBANS project (Dominutti et al., 2025). This supports the idea that OP is a pertinent health metric for PM exposure.

The DTT assay is generally performed offline (Borlaza et al., 2022; Calas et al., 2018), requiring to collect aerosol samples on a filter beforehand. Although offline sampling has certain advantages for conducting chemical analysis, this approach for OP has significant limitations. For instance, the time lag between sampling and analysis prevents the consideration of short-lived species (Fuller et al., 2014), fast-reacting chemical processes (Campbell et al., 2023) and potential aerosol ageing (Ghanem et al., 2024). In addition, reactive species present in the gas phase are not included in OP determination, as offline sampling only considers airborne particles. Online measurements also offer the advantage of providing highly time-resolved data, thus enabling the identification of intermittent sources and/or micro-events responsible for redox activity. Such phenomena can include short-term fluctuations in emission levels, diurnal variations, or rapid changes in wind direction (Campbell et al., 2024).

In recent years, several online systems for measuring aerosol particles OP have been developed to address the limitations of offline methods. Two main operational modes can be distinguished: sequential and continuous. In sequential systems, aerosols

https://doi.org/10.5194/egusphere-2026-4293
Preprint. Discussion started: 30 July 2026

are accumulated over a defined period before the reaction is initiated, after which a time-resolved kinetic analysis of DTT decay is performed (Chen and Yu, 2025; Eiguren-Fernandez et al., 2017; Puthussery et al., 2018; Wu et al., 2022). A significant recent development in sequential online measurement is the ROS-Online prototype, which uses dedicated modules to measure both OP^{DTT} and OP^{AA} simultaneously (Barbero et al., 2025). By contrast, continuous systems, like those developed by Wragg et al. (2016) (ROS^{DCFH}) and Utinger et al. (2023) (OP^{AA}), perform sampling, reaction, and detection in a 'direct-to-reagent' flow. This enables near real-time measurements based on endpoint kinetics. To date, no online instrument implementing the DTT assay has adopted a fully continuous, direct-to-reagent configuration using absorbance spectroscopy. Most existing systems rely on sequential sampling and reaction cycles, which inherently introduce delays between particle collection and analysis. This is particularly problematic for capturing short-lived redox-active species. A recent study reported a loss between 60% and 99% of ROS^{DCFH} and OP^{AA} when comparing online and offline measurements (Campbell et al., 2025). They also demonstrated that ROS^{DCFH} and OP^{AA} values measured online were 5 and 3 times higher, respectively, than those obtained via the fastest offline method, with a 2-min delay between sampling and analysis (Campbell et al., 2025). These findings emphasize that high-time-resolution online measurements of aerosol oxidative potential are critical to capture short-term exposure-relevant variability that is completely missed by offline, time-integrated approaches.

In this context, a continuous DTT system operating with a direct-to-reagent mode can substantially minimize ageing artefacts while providing high temporal resolution, thus enabling the detection of rapid changes in aerosol redox activity. This paper describes the design and first application of a new online instrument for the real-time measurement of the aerosol's OP using the DTT assay and absorbance spectroscopy. The prototype's direct-to-reagent configuration allows continuous, automated monitoring of aerosol redox activity, addressing significant shortcomings in OP^{DTT} instrumentation. Firstly, we evaluated the sensitivity, repeatability, and detection limits of the system by conducting laboratory tests on selected model compounds, such as transition metals and quinones. Secondly, we assessed the system's response to complex pollutant mixtures and photochemically driven processes in an atmospheric simulation chamber (CESAM) (Wang et al., 2011a). The CESAM simulation chamber is labelled as CNRS National Instrument and is part of the ACTRIS European Research Infrastructure (Fuchs et al., 2026). It allows the generation of complex mixtures which are representative of polluted atmospheres for the rigorous evaluation of the OP^{DTT} instrument under controlled conditions. This approach is essential for a new instrument, as it provides a benchmark for its response to complex, dynamically evolving mixtures, a critical step that cannot be achieved through field measurements alone, where sources and meteorology vary simultaneously.

https://doi.org/10.5194/egusphere-2026-4293
Preprint. Discussion started: 30 July 2026

2 Material and methods

2.1 Online OP^{DTT} measurement

2.1.1 Description of the online device

The prototype for the online measurement of DTT consumption induced by aerosols (OP^{DTT}) follows a three-step process involving (i) aerosol sampling, (ii) reaction with a chemical probe, and (iii) analysis (Figure 1). (i) Aerosol sampling is performed using a Particle-Into-Liquid-Sampler (PILS, Model 4001, Brechtel), which collects the aerosols in a liquid phase. (ii) The second step involves two sequential steps. First, the sample reacts with DTT under physiological conditions (phosphate buffer solution, PB, pH 7.4). This leads to DTT oxidation. Secondly, any remaining reduced DTT reacts with DTNB (dithiobis-2-nitrobenzoic acid), forming 2-nitro-5-thiobenzoic acid (TNB), which absorbs at 412 nm. (iii) The third section enables absorbance measurement using a 24 µL measurement cell (Liquid Waveguide Capillary Cells, LWCC-M, WPI) with a 10 cm optical path. This is coupled with a UV-Visible lamp (DH-mini, Ocean Optics) and a spectrophotometer (QE Pro, Ocean Optics). Absorbance at 600 nm is monitored and serves as a reference for temporal drift correction in the absorbance spectra.

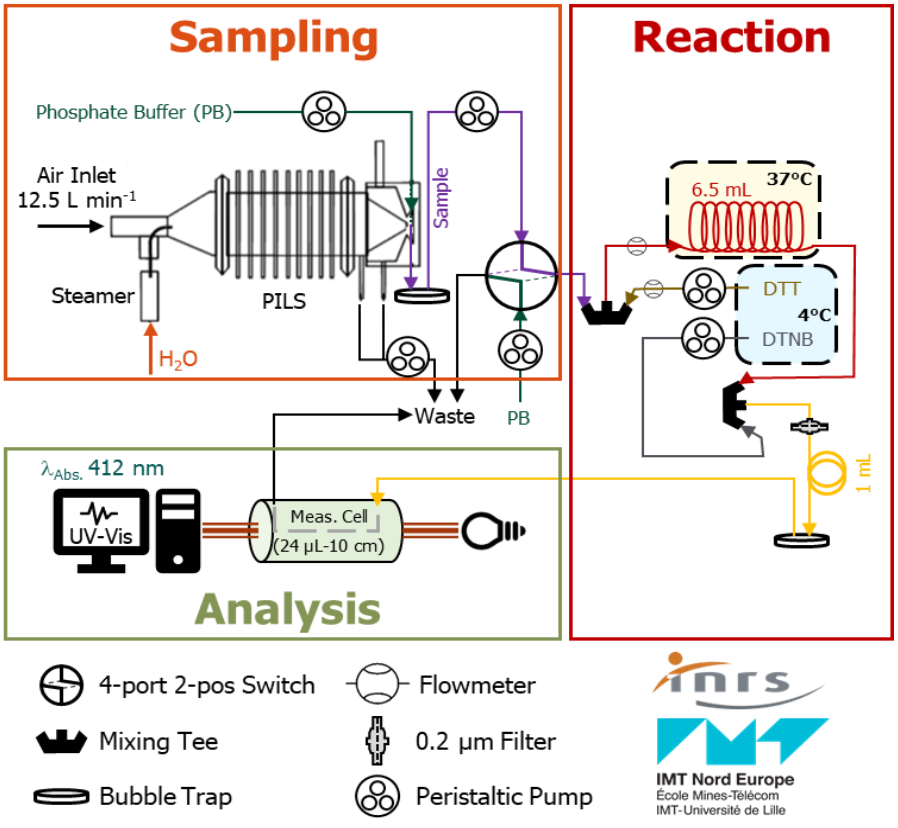

Figure 1: Schematic diagram of the OP^{DTT} online measurement prototype.

https://doi.org/10.5194/egusphere-2026-4293
Preprint. Discussion started: 30 July 2026

The PILS continuously samples air at a flow rate of 12.5 L min^{-1} through a condensation chamber that is fed by a turbulent flow of water vapor at 100°C. Under these conditions of water vapor supersaturation, the aerosols form droplets large enough to be collected by impaction with a collection efficiency for particle diameters D_p between 0.03 and 10 µm greater than 97% (Orsini et al., 2003). The impaction surface is continuously rinsed with phosphate buffer solution (PB, 0.1 mol L^{-1}, pH 7.4) at a flow rate of 0.25 mL min^{-1} to collect the PB-soluble phase of the aerosols. DTT (20 µmol L^{-1}) is injected continuously into the system at a flow rate of 0.25 mL min^{-1} using a microperistaltic pump (29QQ Series, Boxer GmbH). The aerosol sample absorbed in PB (dissolved + particulate fraction) is mixed with the DTT using a mixing tee within the first few seconds after sampling, allowing a direct-to-reagent approach similar to that described by Wragg et al. (2016) and Utinger et al. (2023). This design choice, i.e., delaying the DTT addition, avoids the need for additional dilution factor determination associated with variable PILS condensed water (e.g., using non-interfering tracers such as LiBr ; Sameenoi et al., 2012)), while improving the reproducibility of OP_v^{DTT} measurements. The resulting DTT-aerosol sample mixture then reacts in a 6.3 mL PEEK (PolyEther Ether Ketone) reaction loop, under a constant temperature set at 37°C to mimic human physiology. Liquid flow rates and temperatures are measured continuously using liquid flow meters (SLF3S-0600F, Sensirion®). Unfortunately, the measured reaction temperature (~30°C) was lower than expected during experiments. In the future, we will include enhanced temperature regulations to improve system stability. The effluent is then mixed with DTNB (150 µmol L^{-1}; 0.5 mL min^{-1}), using a second mixing tee before passing through a 1 mL PEEK loop to complete the reaction between DTNB and the remaining DTT. The solution is then filtered through a 0.2 µm syringe filter (Minisart hydrophilic nonsterile syringe filter, Polyamide, 0.2 µm) to prevent clogging the ports of the LWCC-M (Micro Liquid Waveguide Capillary Cell, 100 mm pathlength, WPI) and to remove insoluble particles that could interfere with absorbance measurements through light absorption or scattering. The solution is then injected continuously through the latter to monitor the absorbance spectrum. Absorbance data were averaged over 5-min intervals, which correspond to the response time of the analytical section (see Sect. 2.2.2). This enables the OP to be determined continuously, with a temporal resolution of 5 minutes and a 20-min lag between air sampling and analysis of TNB absorbance. DTT ageing is limited by protecting it from light (stored in an amber bottle) and keeping it cold (below 4°C) using ice and a thermoregulated bottle holder. A 4-port, 2-position switch valve (Advanced Microfluidics®) allows for a blank sample (PB) to be periodically injected into the reaction loop instead of the aerosol sample to perform analytical blanks and control the stability of the DTT.

2.1.2 Comparison with literature

Table 1 provides a list of online instruments based on the DTT assay, their limit of detection, operational mode and their sampling devices. These instruments follow the same three-step process as described previously. Various aerosol sampling systems have been employed, attempting to improve the representativeness of the atmospheric aerosol sample while ensuring that they collect a sufficient quantity for OP determination. The choice of a sampler significantly impacts the collection efficiency, particularly for ultrafine particles as well as air flow rates. The latter remain key design variables in the development of online OP instruments (Table 1).

https://doi.org/10.5194/egusphere-2026-4293
Preprint. Discussion started: 30 July 2026

The different samplers include the Sequential Spot Sampler (Eiguren Fernandez et al., 2014; Eiguren-Fernandez et al., 2017), which condenses water on aerosols forming discrete liquid spots for later reaction; the Mist Chamber Collector (Cheung et al., 2024; Puthussery et al., 2018), which traps particles in an aqueous phase through condensation-enhanced impaction; and the MARGA system. The latter draws air through a wet rotating denuder followed by a steam-jet aerosol collector, enabling the dissolution of both gaseous and particulate species into separate liquid streams for subsequent analysis (Wu et al., 2022). The BioSampler uses laminar-flow water condensation to efficiently capture airborne particles in a liquid medium while limiting the loss of volatile and reactive compounds (Barbero et al., 2025). Finally, the PILS (see description in section 2.1.1) is one of the most widely adopted systems for DTT (Chen and Yu, 2025; Koehler et al., 2014; Sameenoi et al., 2012) as well as other OP assays (Utinger et al., 2023; Wang et al., 2011b). Although PILS sampling relies on a turbulent injection of water vapor at 100°C, Utinger et al. (2023) reported that temperatures within the condensation chamber (~35-40°C) do not significantly impact OP-active species.

Table 1. List of OP^{DTT} online measurements and their sampling characteristics. $[DTT]_r$ refers to the initial DTT concentration used in the reaction between the sample and DTT.

Aerosol sampler (reference)	Sample flow rate (L min^{-1})	Aerosol collection efficiency	Air-to-liquid ratio (m^3_{air} mL^{-1})	Time resolution (min)	Operational mode	$[DTT]_r$ (µmol L^{-1})	LOD ($nmol_{DTT}$ min^{-1})
Sequential Spot Sampler (Eiguren-Fernandez et al., 2017)	3.0	> 90% (0.02 – 1 µm)	1.08	180	Sequential	100	0.15
Mist chamber (Cheung et al., 2024; Puthussery et al., 2018)	16.7 or 42	"Similar to PILS" (King and Weber, 2013)	0.38 – 2.88	60	Sequential	100	0.24 (Puthussery et al., 2018) 0.19 – 0.49 (Cheung et al., 2024)
MARGA (Wu et al., 2022)	16.7	> 99% (0.019 – 0.886 µm) (Khlystov et al., 1995)	0.04	60	Sequential	71	0.024
BioSampler (Barbero et al., 2025)	10.5	40 % (0.05 – 0.08 nm) > 90% (0.5 – 5 µm)	0.001	60	Sequential	212	0.025
PILS (Chen and Yu, 2025)	16.7	> 97% (0.03 – 10 µm)	0.05	60	Sequential	100	0.270 [a]
PILS (Koehler et al., 2014; Sameenoi et al., 2012)	12.5	> 97% (0.03 – 10 µm)	Not mentioned	3	Continuous [b]	50	0.001 [c]
PILS (This study)	12.5	> 97% (0.03 – 10 µm)	0.05	5	Continuous	10	0.066

[a] Calculated using detection limit of 0.027 µM min^{-1} and considering the DTT incubation solution volume of 10 mL [35]
[b] This instrument relies on a microfluidic electrochemical sensor
[c] Calculated using detection limit of 24.9 $pmol_{DTT}$ per injection and considering the 18 min time residence in the system [43,47]

https://doi.org/10.5194/egusphere-2026-4293
Preprint. Discussion started: 30 July 2026

The main distinction among these samplers lies in their particle collection efficiency, particularly for sub-500 nm particles, and in their air-to-liquid ratio, which determines the sample dilution. Instruments such as the MARGA and PILS exhibit consistently high collection efficiencies (> 97%) for a large particle size range. The air-to-liquid ratio extends over a range of more than two orders of magnitude across the various instruments, from 0.001 m^3_{air} mL^{-1} for the BioSampler to 1.08 m^3_{air} mL^{-1} for the Sequential Spot Sampler. A higher ratio enhances the transfer of particles and reactive species in the liquid sample making it a critical variable in the design of continuous systems.

Table 1 also reports the initial DTT concentration ($[DTT]_r$) used in the reaction between the aerosol sample and DTT, which varies among published online systems, ranging from 50 to 212 µmol L^{-1}. Notably, Sameenoi et al. (2012) evaluated several initial DTT concentrations across different 1,4-naphthoquinone concentrations and found that lower initial DTT concentrations resulted in higher analytical sensitivity. This not only highlights the absence of a standardized operating protocol for online OP^{DTT} measurements, but also emphasizes the need to interpret cautiously direct comparisons between online measurements. The different online systems exhibit limits of detection (LODs) ranging from 0.001 nmol min^{-1} for the microfluidic electrochemical sensor to 0.49 nmol min^{-1}. The instrumental LOD of our system was calculated as three times the standard deviation of the continuous signal obtained under HEPA-filtered air (blank) conditions. Across the 11 blanks (>10 min) performed over two consecutive days, the mean LOD was 0.066 ± 0.016 nmol min^{-1} (ranging from 0.038 to 0.088 nmol min^{-1}).

Previous OP^{DTT} online systems described in Table 1 rely on sequential sampling (with the exception of the Sameenoi et al. system) with accumulation times typically ranging from 20 to 60 minutes. During this interval, rapid fluctuations in OP cannot be observed, and short-lived reactive species may be partially lost before reaction with DTT can occur, as highlighted for ROS^{DCFH} and OP^{AA} by (Campbell et al., 2025). The configuration of our OP^{DTT} online measurement system overcomes this limitation and provides an advantageous balance: while maintaining a competitive LOD, it allows the continuous measurement of OP^{DTT} with a high temporal resolution of 5 minutes. This enables the detection and characterization of short-lived events that would remain unresolved with traditional hourly or multi-hourly sampling approaches. This enhanced temporal resolution is particularly relevant for capturing rapid changes in aerosol OP during transient photochemical or combustion-related episodes, possibly involving short-lived oxidative species.

2.2 Evaluation strategy

2.2.1 Reagents and chemical preparation

The PB solution was prepared at a total phosphate concentration of 0.1 mol L^{-1} from 0.02 mol L^{-1} KH_2PO_4 (99%, Sigma-Aldrich) and 0.08 mol L^{-1} K_2HPO_4 (98%, Sigma-Aldrich) in ultrapure water (Milli-Q®, 18.2 MΩ.cm, TOC < 5 ppb) to obtain a pH of 7.4 ± 0.1. If needed, pH is adjusted using HNO_3 (67%, ultrapure, VWR international).

https://doi.org/10.5194/egusphere-2026-4293
Preprint. Discussion started: 30 July 2026

DTT (Cleland reagent, 1,4-dithiothreitol, Roche Diagnostics GmbH) and DTNB (Ellman reagent, 5,5′-dithiobis-2-nitrobenzoic acid 99%, Sigma Aldrich) stock solutions were prepared in PB at concentrations of 1 mmol L^{-1}. Before each experiment, DTT and DTNB solutions were diluted to 20 and 150 µmol L^{-1}, respectively.

1,4-NQ (1,4-naphthoquinone, Fluka puriss p.a. > 98.5%) and 9,10-PQ (9,10-phenanthraquinone, Sigma Aldrich, 99%) were dissolved in absolute methanol (Biosolv) to prepare stock solutions at 492.5 and 495 µmol L^{-1} in amber bottles. Cu^{2+} ($CuSO_4.5H_2O$, Merck, Emprove, > 98.5%) was dissolved in PB to prepare stock solutions at 500 µmol L^{-1} in a PFA bottle. Target concentration solutions (Table 2) were prepared by diluting the stock solution with PB solution prior to experimentation.

2.2.2 Laboratory sensitivity tests

The online OP measurement device has been tested in the laboratory using various model compounds. These compounds are redox-active organic and metal compounds that were selected based on those reported in the literature as key reactive species for the DTT test (Charrier and Anastasio, 2012; Kumagai et al., 2002). The sensitivity of the system was determined by injecting the model compounds at five different concentrations listed in Table 2 into the online system. Injection is carried out by bypassing the PILS at the 4-way 2-position valve (Figure 1) and begins with a blank (PB), gradually increasing the concentration of a given model compound. A blank test with PB is performed between each new concentration to correct for any progressive increase associated with DTT ageing using linear regression. Each test was repeated 3 times. This allowed us to determine the response functions between DTT consumption (OP^{DTT} in nmol min^{-1}) and the concentrations of the various model compounds, as well as the determination of the linear range of the latter.

Table 2. Concentration tested for each model compound.

Model compound	Concentration range (µmol L^{-1})
9,10-PQ	0.06, 0.12, 0.48, 0.95, 1.9
1,4-NQ	0.05, 0.1, 0.5, 1, 5
Cu (II)	0.1, 0.5, 1, 5, 10

The response time (t_R) of the analytical section was determined through using model compounds. It was defined as the time required for the absorbance to change from 10% to 90% of the total variation towards the final steady state following a change in the input (either PB or the model compounds). The measured t_R values ranged from 90 to 300 s, with faster responses observed for larger absorbance variations. For subsequent calculations, the longest t_R (5 min) was used.

https://doi.org/10.5194/egusphere-2026-4293
Preprint. Discussion started: 30 July 2026

2.2.3 Simulation chamber measurements

The second stage of evaluation of the online OP measurement system was carried out in the CESAM atmospheric simulation chamber (French acronym for Experimental Multiphasic Atmospheric Simulation Chamber; https://cesam.cnrs.fr/; (Wang et al., 2011a). CESAM is a 4.2 m^3 stainless steel reactor used to generate controlled and/or realistic concentrations of air pollutant mixtures (particles and gases) (Georgopoulou et al., 2024).

The setup is displayed in Figure 2. The experimental protocol involved the continuous injection of carefully selected mixtures of primary pollutants in order to simulate a complex urban atmosphere with primary and secondary species. For gases, primarily nitrogen monoxide (NO) and biogenic and anthropogenic volatile organic compounds (VOCs) were injected, i.e., methylglyoxal (Sigma Aldrich), toluene (R.P. Normapur®, PROLABO), m-xylene (Touzart & Matignon), tridecane (Sigma Aldrich, > 99%), and α-pinene (Sigma Aldrich, > 97.5%). For particles, black carbon (BC) was generated via the combustion of wood pellets in a controlled oven setup at 400°C to simulate biomass burning sources. The BC generation occurs within a buffer chamber (namely "Pellets chamber"), which enables the injection of particles into the CESAM chamber in defined pulsed sequence. Transition metals (Fe, Cu, and Mn), characteristic of vehicular non-exhaust emissions (Birmili et al., 2006; Pant and Harrison, 2013), were introduced using an atomizer (TSI, model 3075) with an aqueous solution of 50, 2.5 and 2.5 µmol L^{-1} of $FeSO_4.6H_2O$ (R.P. Normapur® PROLABO, 99%), $CuSO_4.5H_2O$ (Aldrich, > 98%), and $MnSO_4{\cdot}H_2O$ (Rectapur®, 99%), respectively. Ammonium sulfate $(NH_4)_2SO_4$ (Sigma Aldrich, 99.9999%), was also injected by atomizing an aqueous solution of 2.5 mmol L^{-1} to promote the nucleation and growth of secondary organic aerosols (SOA). Photochemical reactions, initiated by three 6.5 kW high-pressure arc xenon lamps (MH Diffusion® MacBeam™ 4000) in the presence of NO and VOCs, led to the formation of ozone (O_3), SOA, and other reactive species (e.g., OH, H_2O_2 ; Badali et al., 2015; Manfrin et al., 2019) that are not analyzed. To observe the cumulative effect of atmospheric pollutants on OP, experiments began with a simple initial pollutant mixture, to which species were progressively added, and their concentrations increased. This design enabled the evaluation of the OP^{DTT} response to increasingly more complex pollutant mixtures and photochemically driven processes under conditions approaching those of real ambient air scenarios.

Aerosol particle size distribution between 5 and 800 nm was measured using a DMPS (Differential Mobility Particle Sizer, Tropos). The number of particles was determined using a CPC (Condensation Particle Counter, CPC 3750, TSI). The chemical composition of non-refractory (NR) PM_1 particles was monitored using a ToF-ACSM (Time-of-Flight Aerosol Chemical Speciation Monitor, Aerodyne). The mass concentration of particles was determined from DMPS measurements by using the average density calculated with ToF-ACSM measurements. Black carbon was measured using an aethalometer (AE33, Magee Scientific). Metal concentrations were obtained using an Xact® 625i (Cooper Environmental). The OP^{DTT} online measurement system was connected directly to the simulation chamber via a 3-way manifold. Particle-free OP^{DTT} blanks were performed by pumping air through a HEPA filter (Fig. S1). Regarding the gas-phase composition, the mass concentrations of O_3, nitrogen oxides (NO_X) and sulfur dioxide (SO_2) were measured using Horiba® analyzers.

https://doi.org/10.5194/egusphere-2026-4293
Preprint. Discussion started: 30 July 2026

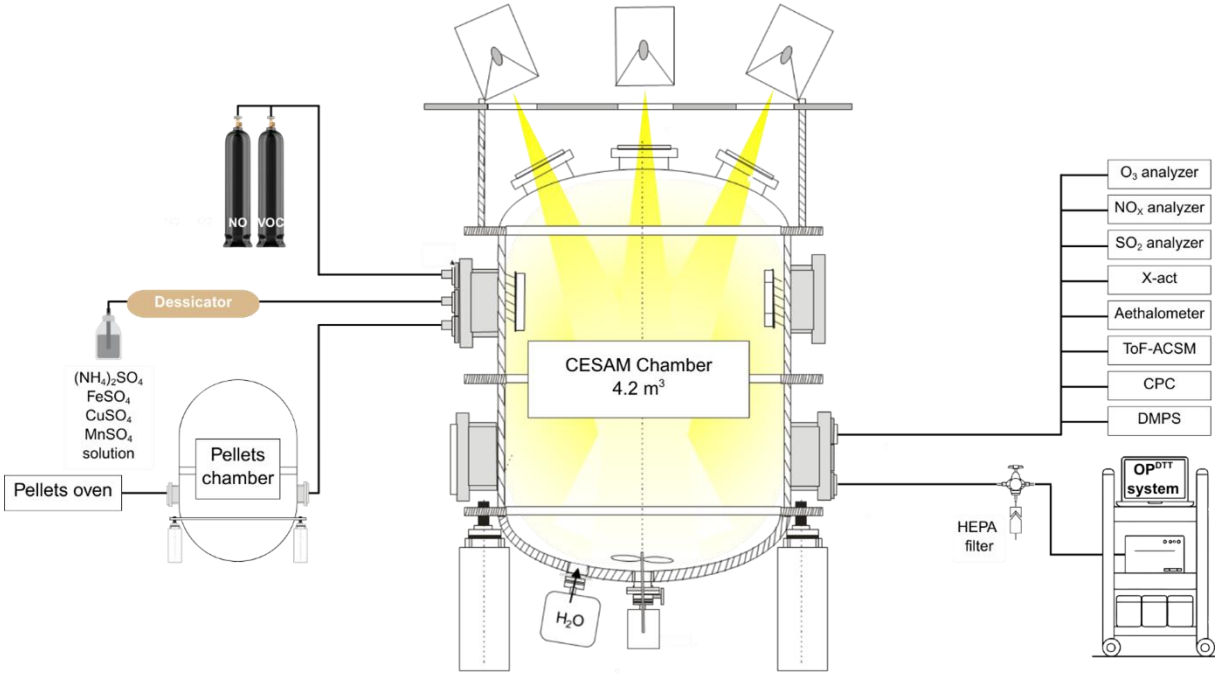

Figure 2. Schematic diagram of the CESAM chamber setup.

2.2.4 Calculation of OP

In the absence of harmonized protocols for measuring OP^{DTT}, particularly for online measurement techniques, it is challenging to produce results that can be consistently compared with those in the existing literature. To address this issue, we express our laboratory results as DTT consumption through the OP^{DTT} (nmol min^{-1}) using Equation (1):

$$OP^{DTT}(nmol\ min^{-1}) = f \times \frac{(PB\ Abs - Sample\ Abs)}{Slope\ (mL\ mol^{-1})} \times Reaction\ Liquid\ Flow\ Rate\ (mL\ min^{-1}), \quad (1)$$

Where: f is the dilution factor introduced by the addition of DTNB prior to absorbance measurement (f = 2), "PB Abs" is the absorbance of the analytical blank (412 nm corrected using the 600 nm absorbance), estimated at the time of sample analysis using linear regression of successive blank measurements to correct for DTT ageing; "Sample Abs" is the corresponding baseline-corrected absorbance of the sample ; the slope of the calibration curve corresponds to the relationship between absorbance and DTT concentration in the LWCC; and the reaction liquid flow rate is 0.5 mL min^{-1}.

We further express an air volume-based OP_v^{DTT} (nmol min^{-1} m^{-3}) as a function of the air sampling volume (V_{air}, m^3), calculated as the air sampling flow rate of the PILS multiplied by the response time (t_R) of the system (see section 2.2.2) using Equation (2):

https://doi.org/10.5194/egusphere-2026-4293
Preprint. Discussion started: 30 July 2026

$$OP_v^{DTT} = \frac{OP^{DTT}}{V_{air}}, \quad (2)$$

The OP_v^{DTT} is thus the number of moles of DTT oxidized per minute for one cubic meter of air.

This approach provides a robust framework for quantifying OP_v^{DTT} under variable atmospheric conditions. It also contributes to the establishment of a standardized method for continuous online OP measurements.

An explanatory analysis was conducted to identify parameters that most strongly influence the observed OP_v^{DTT}. To achieve this, a multiple linear regression was applied using OP_v^{DTT} values and chemical data obtained from the simulation chamber measurements. All calculations were performed using the scikit-learn library in Python.

3 Results and discussion

3.1 Laboratory sensitivity tests

Laboratory blank tests were conducted using PB solutions. The resulting DTT consumption rate in PB blanks averaged 0.062 ± 0.018 nmol min^{-1}.

Figure 3 illustrates the sensitivity of our online OP^{DTT} instrument towards different species. It shows the linear relationship between the DTT consumption rate and the concentrations of 9,10-PQ, 1,4-NQ, and Cu (II). The same laboratory test was performed, with Fe (III) concentrations ranging up to 50 µmol L^{-1}, but no significant reactivity was observed. The reported concentrations correspond to the those injected into the system. Each concentration level was analysed in triplicate to assess measurement repeatability. The homogeneity of variance between the triplicate datasets was confirmed with 99% confidence (Cochran's test) for both 9,10-PQ and Cu (II) across the tested concentration ranges. By contrast, measurements for 1,4-NQ at a low concentration (0.05 µmol L^{-1}) did not meet the criteria of Cochran's test at the 99% confidence level and were therefore discarded. The measured DTT consumption rates are lower than those previously reported in the literature (e.g., Charrier and Anastasio, 2012; Ghanem et al., 2021). For example, Charrier and Anastasio (2012) reported a DTT consumption rates of 0.88 μmol_{DTT} L^{-1} min^{-1} and 0.71 ± 0.09 μmol_{DTT} L^{-1} min^{-1} for 1 µM of Cu (II) and 0.05 µM of 9,10-PQ, respectively. Given the 3 mL reaction volume, this corresponds to 2.64 $nmol_{DTT}$ min^{-1} and to 2.13 ± 0.27 $nmol_{DTT}$ min^{-1} for Cu (II) and 9,10-PQ, respectively. This discrepancy is likely attributable to differences in the assay's conditions, including the initial DTT concentration, which is known to affect reaction kinetics (Lin and Yu, 2019), as well as the sensitivity of the analytical method (Sameenoi et al., 2012). Nevertheless, assuming initial rate of DTT loss remains proportional to the concentrations of redox-active species, the response remained linear within the following ranges: between 0.06 and 0.95 µmol L^{-1} for 9,10-PQ, from 0.1 to 5 µmol L^{-1} for 1,4-NQ, and between 0.1 and 10 µmol L^{-1} for Cu (II). Notably, 9,10-PQ showed a higher reactivity with DTT compared to 1,4-NQ, which is consistent with previous literature (Charrier and Anastasio, 2012).

Based on the regressions, we calculated analyte-specific LODs (µmol L^{-1}) of the measurement system for each compound as three times the intercept uncertainty divided by the slope (Miller and Miller, 1993). To convert these values to equivalent

https://doi.org/10.5194/egusphere-2026-4293
Preprint. Discussion started: 30 July 2026

atmospheric concentrations (µg m^{-3}), we accounted for the PILS sampling, rinsing flow rates and its sampling efficiency (Sect. 2.1.1). The resulting LODs were 0.02, 0.18, and 2.0 µmol L^{-1} for 9,10-PQ, 1,4-NQ, and Cu (II), respectively, corresponding to 0.09, 0.56, and 2.56 µg m^{-3} in the atmosphere. For each analyte, a linear response of DTT consumption was observed over the concentration ranges tested in the laboratory (9,10-PQ: 0.09–4.28 µg m^{-3}; 1,4-NQ: 0.56–15.6 µg m^{-3}; Cu (II): 2.56–12.8 µg m^{-3}), with no deviation from linearity within these ranges. No saturation of the DTT response was observed within the tested concentration ranges for Cu and 1,4-NQ. However, for 9,10-PQ, deviation from linearity was observed at the highest concentrations tested, indicating that the upper limit of the linear dynamic range was reached under these conditions (atmospheric-equivalent concentration of 8.55 µg m^{-3}).

The atmospheric-equivalent LODs are relatively high compared to the ambient concentrations observed at various urban locations in Europe (Liu et al., 2024; Pietrogrande et al., 2022; Ringuet et al., 2012) (Cu: 5-20 ng m^{-3}; see supplementary Tables 3 and 4 in Mishra et al. (2026) for 1,4-NQ: < 0.47 ng m^{-3} and 9,10-PQ: < 1.20 ng m^{-3}). However, these copper concentrations can be observed in some micro-environments such as railway environments (2.52 µg m^{-3} ; Queron et al., 2022) or in some occupational settings (smelters: 120 µg m^{-3} ; Haase et al., 2021). However, the upper limit of linearity for 9,10-PQ was reached during experiments.

The reproducibility of these results on both analytical blanks and model compounds serves as a proof of concept of the prototype's functionality. However, it is important to note that the obtained LODs for model compounds correspond to relatively high atmospheric concentrations compared to actual ambient levels. In addition, it should be acknowledged that under real operative conditions, DTT decay is the results of the reactivity of a complex mixture and not only an isolated compound as tested here.

https://doi.org/10.5194/egusphere-2026-4293
Preprint. Discussion started: 30 July 2026

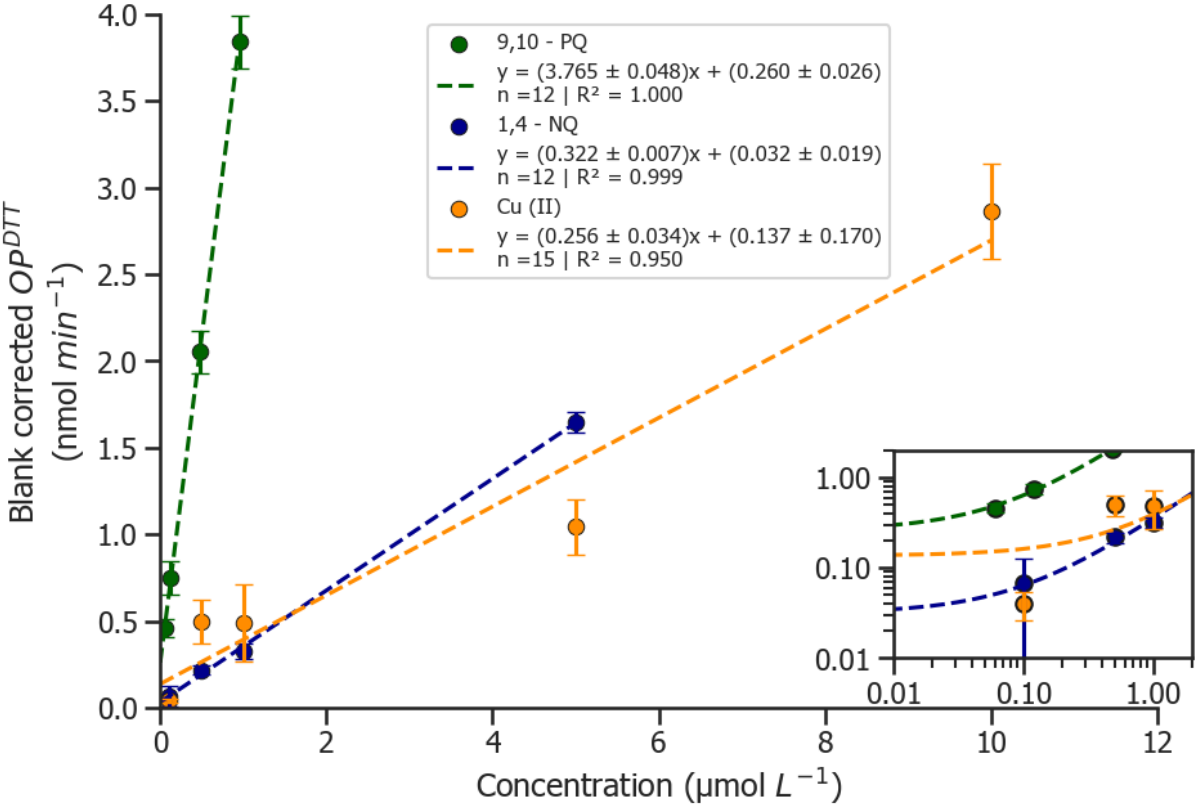

Figure 3. Blank corrected OP^{DTT} (nmol min^{-1}) as a function of concentration of redox-active species (9,10-PQ in green, 1,4-NQ in blue and Cu (II) in orange). Error bars correspond to the standard deviation of the three replicates and the dotted line to the linear regressions. The box in the lower right shows a zoomed view of the range from 0.01 to 2 on a logarithmic scale, thus linear regressions appear curved.

3.2 Simulation chamber measurements

The online measurement device was tested for continuous online measurements of several sources in the CESAM simulation chamber. Although our prototype measures OP_v^{DTT} with a resolution time of 5 minutes (Fig. S2), all datasets were reprocessed and at a unified temporal resolution of 15 minutes to enable a comprehensive analysis. This was done according to the lowest time resolution of other analytical instruments (i.e. 15 minutes for online metal analysis).

Figure 4 displays the time-resolved OP_v^{DTT} alongside the number and mass concentrations of particles, the chemical characterization of the simulated atmospheric environment including redox-active metals, BC concentrations, and the relative proportions of chemicals in the NR-PM_1. This representation illustrates how OP_v^{DTT} evolves dynamically in response to increasing pollutant concentrations, mixing, and ageing. Grey shaded areas indicate OP_v^{DTT} blank measurements (HEPA-filtered air sampling). The corresponding raw absorbance data are shown in Fig. S1.

https://doi.org/10.5194/egusphere-2026-4293
Preprint. Discussion started: 30 July 2026

The experiment (Figure 4, April 16) began with the injection of Cu, VOCs, NO, and $(NH_4)_2SO_4$ seed particles into the simulation chamber. Photochemical reactions were then triggered by activating UV lamps, resulting in the formation of SOA, O_3, and potentially other reactive species (including unanalyzed radicals). Following an initial stabilization period (~90 min), the simulated atmosphere exhibited an O_3 concentration of 90 ± 4 ppb and a PM_1 mass concentration around 41 µg m^{-3}. The NR-PM_1 fraction was predominantly composed of organic matter (70%) and sulfate (18%). BC was present at a concentration of around 260 ng m^{-3}, and Cu was at 17 ng m^{-3}. Iron (Fe) concentration is neither discussed nor presented in Figure 4, since laboratory calibration has shown that Fe does not induce significant DTT consumption.

Under these initial conditions, the OP_v^{DTT} value ranged between 5.20 ± 0.03 and 6.61 ± 0.02 nmol min^{-1} m^{-3}. Beginning at 13:00, Mn was progressively injected, reaching 15 ng m^{-3} by 15:00. Organic aerosol (OA) concentrations also increased from 28 to 35 µg m^{-3}. This coincided with an increase in OP_v^{DTT} to 8.69 ± 0.05 nmol min^{-1} m^{-3}, while O_3 and Cu concentrations decreased. These changes suggest a compensatory oxidative contribution from Mn and/or OA.
From 16:00 to 18:30, the OP_v^{DTT} increased to 12.98 ± 0.04 nmol min^{-1} m^{-3}, concomitant with a continuous increase of OA and BC concentrations up to 61 µg m^{-3} and 680 ng m^{-3}, respectively. After a slight increase, Cu and Mn concentrations remained stable. During this period, the total number of particles and O_3 levels remained relatively stable, supporting the hypothesis that the increase in OP_v^{DTT} was primarily driven by high levels of OA and BC concentrations, with some contribution from redox-active metals. After 18:30, OP_v^{DTT} displayed a decreasing trend down to 9.88 ± 0.03 nmol min^{-1} m^{-3}, concomitant with a small decrease in redox-active metals, while OA mass concentration, BC, and O_3 levels remained stable.

In a subsequent experiment (Figure 4, April 17), no VOCs were injected, and UV lamps were not activated. Therefore, the simulation chamber was devoid of SOA (OA < 35% of NR-PM_1 and < 22 µg m^{-3}), ozone (O_3 < 5 ppb), and reactive species photochemically produced. The presence of OA can be attributed to the injection of BC from the combustion of wood pellets as a pulse between 11:00 and 14:00 (not shown on Figure 4 for 17/04). Despite an initial atmosphere containing elevated levels of BC (546 ± 48 ng m^{-3}) and Cu (40 ± 5 ng m^{-3}), lower OP_v^{DTT} values were measured, around 2.48 ± 0.07 nmol min^{-1} m^{-3}. OP_v^{DTT} increased until 17:00, up to 4.38 ± 0.04 nmol min^{-1} m^{-3}, in line with the increase in Mn concentration (from 0 to 14 ng m^{-3}), PM_1 mass concentration (from 62 to 70 µg m^{-3}) as well as a decrease of OA proportion (from 35% to 25%), due to the pulse injection of BC and the dilution of the chamber. After 17:00, however, the OP_v^{DTT} values remained stable while Mn and Cu concentrations increased up to 50 ng m^{-3} and the OA proportion decreased to 20%.

https://doi.org/10.5194/egusphere-2026-4293
Preprint. Discussion started: 30 July 2026

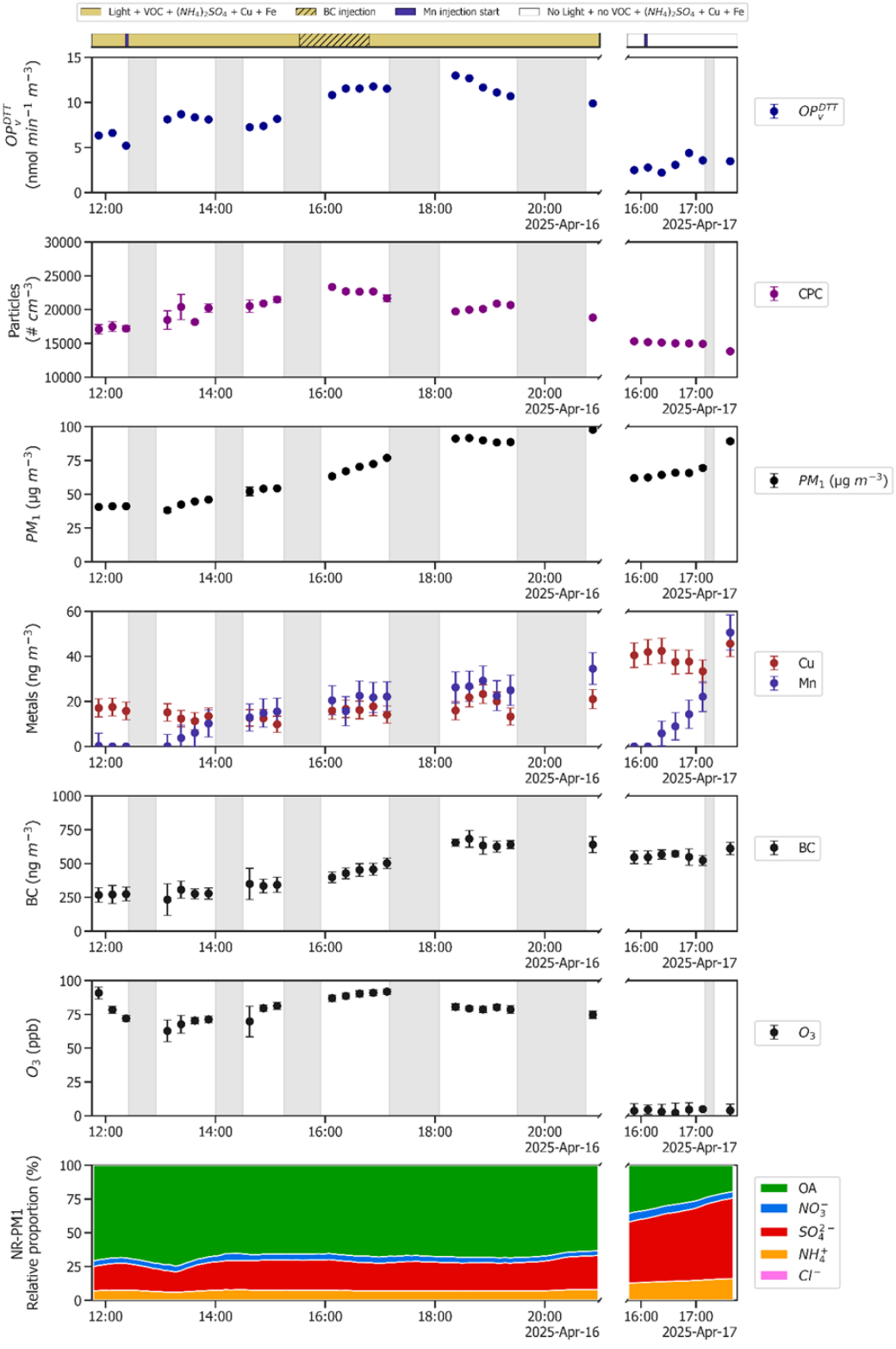

https://doi.org/10.5194/egusphere-2026-4293
Preprint. Discussion started: 30 July 2026

Figure 4. Time-resolved OP_v^{DTT} and chemical characterization of the simulated atmospheres in the CESAM chamber for two consecutive days: photochemical experiment on the left and non-photochemical experiment on the right, separated by slashes. Grey shaded areas indicate OP_v^{DTT} blank measurements (HEPA-filtered air sampling). Points show the 15-min average with standard deviation error bars. For OP_v^{DTT}, error bars represent the 95% confidence interval of 15-min averaged value, computed from 1 Hz measurements using the t-student test. An increasing trend of OP_v^{DTT} is observed during the photochemical experiment along with an increase of PM_1 and transition metal mass concentrations, while the non-photochemical experiment shows lower values while displaying similar to higher levels of PM_1 and transition metal mass concentrations but lower levels of ozone and organic aerosol (OA). This contrast illustrates the central role of photochemical processes in driving aerosol oxidative potential.

3.3 Discussion on photochemistry and OP sensitivity

OP_v^{DTT} values obtained under non-photochemical conditions (April 17) remained consistently lower than those measured during experiments involving active photochemistry (April 16), despite higher concentrations of redox-active metals and similar PM_1 mass concentrations. Two hypotheses have been postulated to explain these observed differences: first, a direct effect of decreasing O_3 concentrations; and second, an absence of photochemically produced species. To investigate this, we conducted dedicated experiments on a controlled test bench generating O_3 and NO_2 under stable conditions (Ghazaly, 2019). Over the tested concentration range (O_3: 0–120 ppb; NO_2: 0–520 ppb), no measurable DTT decay was observed, suggesting that neither O_3 or NO_2 directly contribute to DTT consumption under these conditions. This emphasizes the additional contribution of photochemically produced species such as SOA as well as the hydroxyl (OH), hydroperoxy (HO_2), and organic peroxy (RO_2) radicals, to the total oxidative potential (Campbell et al., 2024; Jiang and Jang, 2018; Tuet et al., 2017)[39,65,66].

During the photochemical experiment, OP_v^{DTT} exhibited a decreasing trend towards the end of the experiments, although OA proportion and PM_1 concentration levels were stable. Since BC was injected as a pulse (Figure 2), it is possible that the associated reactive species such as quinones underwent ageing processes resulting in lower intrinsic reactivity, as previously suggested by Jiang and Jang (2018). In addition, although O_3 levels remained relatively constant after 18:00, concentrations decreased slightly in comparison with 16:00-18:00 values (from 90 to 80 ppb), which may reduce formation rates of reactive species, which could explain the lower OP_v^{DTT} measured. Such rapid variations in OP_v^{DTT} are expected under real urban conditions (traffic plumes, photochemical episodes), highlighting the limitations of 24 h-integrated offline approaches for exposure assessment.

In contrast, during the non-photochemical experiment, our results align with the known redox activity of manganese and copper, which has been shown to contribute significantly to DTT consumption (Charrier et al., 2015, 2016; Charrier and Anastasio, 2012; Ghanem et al., 2021). Yet, despite their elevated concentrations, OP_v^{DTT} appears to have reached a plateau, as recently observed for Cu by Barbero et al. (2025). This behavior may be attributed to a saturation effect, as previously described for Cu (II) and Mn (II), reflecting the nonlinear nature of DTT-metal reactivity (Charrier et al., 2016; Charrier and Anastasio, 2012; Ghanem et al., 2021). A two-stage kinetics involving formation of [DTT-Cu] complex (Kachur et al., 1997), may also contribute to limiting its reactivity with DTT.

https://doi.org/10.5194/egusphere-2026-4293
Preprint. Discussion started: 30 July 2026

To complement this interpretation, we conducted a multiple linear regression analysis on the dataset from the CESAM simulation experiments. The limited number of data points and the collinearity between the parameters prevent us from interpreting the model correctly. Nevertheless, analysis of the bivariate relationships reveals that OA mass concentration is the main driver explaining the variance (> 80%) in OP_v^{DTT}. This result further supports the predominant role of photochemically derived organic species in driving the oxidative potential of the aerosol.

3.4 Limitations and operational considerations

It must be noted that the actual design of our instrument does not account for potential absorption by chromophoric components at 412 nm (e.g., brown carbon ; Basnet et al. 2024). Such species may contribute to the measured absorbance independently of DTT consumption, potentially leading to an increase of the DTT concentration and thus an underestimation of OP_v^{DTT}. This effect was not explicitly corrected for in the present study and therefore represents a limitation of the current system. Future developments will include multi-wavelength approaches or direct sample absorption measurement to better constrain matrix absorption.

Due to the use of PILS sampling, water-soluble gaseous species may also be incorporated into the liquid phase and contribute to the measured OP_v^{DTT}. While our results suggest that neither O_3 or NO_2 directly contribute under the tested conditions, the potential contribution of other reactive gas-phase species cannot be excluded. Therefore, the measured OP_v^{DTT} should be interpreted as an integrated signal reflecting both particulate and dissolved gas-phase species. Future work will also focus on quantifying the respective contributions of water-soluble gaseous species and particulate matter to the total OP_v^{DTT} signal by performing complementary measurements under particle-free conditions (using HEPA filter) gas-free conditions (using denuders).

The stability of the DTT reagent was monitored throughout the day by performing regular blank measurements, including filtered air blanks and analytical blanks, using a 4-way, 2-position switch valve (see Sect. 2.1.1). This methodology facilitates the monitoring of DTT ageing over time, and the resulting signal drift was corrected using linear regression.

Regarding system maintenance, routine cleaning procedures were implemented to ensure stable operation and minimize contamination. The system was thoroughly rinsed with ultrapure water (Milli-Q®, 18.2 MΩ.cm, TOC < 5 ppb) and PB prior to and at the end of each measurement day. In addition, an acid cleaning step was performed before and after each measurement campaign using a diluted nitric acid solution (0.05% v/v, from 67% ultrapure HNO_3, VWR International) to remove any potential metal residues and prevent memory effects. Inline filters were also replaced on a daily basis to avoid particle accumulation. These procedures ensured stable baseline conditions and contributed to the overall reproducibility of OP_v^{DTT} measurements.

https://doi.org/10.5194/egusphere-2026-4293
Preprint. Discussion started: 30 July 2026

The present configuration allows OP_v^{DTT} measurements at high-temporal resolution (5-min), but requires continuous reagent supply. Under pre operating conditions, the system can run autonomously for 20 hours, after which reagents (DTT, DTNB and PB) must be replenished. As a result, the instrument is presently better suited for event-based studies, rather than for long-term autonomous deployment in routine regulatory or epidemiological monitoring. However, the system autonomy can be extended by optimizing operational parameters, such as reducing flow rates and increasing reagent reservoir volumes, and ongoing efforts are directed toward improving long-term stability and operational robustness.

4 Conclusion

The inclusion of OP in the new European air quality directive marks a significant turning point in air quality policy (European Parliament, 2024). Regulatory attention is increasingly focused on aerosol toxicity, acknowledging that not all particles have comparable health implications, and that some can exhibit high reactivity, even at low concentrations (Kelly and Fussell, 2012). In this context, a new online system for measuring oxidative potential has been developed. It is based on the dithiothreitol assay (OP_v^{DTT}) and the direct-to-reagent approach. This system facilitates real-time assessment of the OP_v^{DTT}, with high temporal resolution, eliminating the need for offline sample processing.

The system successfully monitored the OP_v^{DTT} under transition metal concentrations (e.g., Cu and Mn), BC, and O_3 levels within ranges commonly reported for European urban environments (e.g., < 20 ng m^{-3} for Cu and Mn ; Poulakis et al., 2015). Although PM_1, ranging from 38 to 98 µg m^{-3}, and organic aerosol levels exceeded the European urban average background, they remained consistent with the ranges reported in Asian megacities (Huang et al., 2014; Liu et al., 2012; Yang et al., 2022) or during pollution events in Europe (Bressi et al., 2016).

Beyond method development, the present study provides new insights into the drivers and dynamics of aerosol OP under controlled yet atmospherically relevant conditions. Chamber experiments revealed that OP_v^{DTT} is strongly influenced by photochemical processes, with significantly higher values observed under conditions promoting secondary formation compared to experiments without photochemistry. This controlled environment enabled us to move beyond simple correlations and directly attribute changes to specific additions of pollutants (Mn as an illustration) or the activation of photochemical processes. This provide a mechanistic understanding of the instrument's response that is impossible to obtain from ambient field data. This emphasizes the substantial role of photochemically produced species in driving OP_v^{DTT}, even in the presence of redox-active metals such as Cu and Mn. The high temporal resolution (5-minutes) of the system facilitates a more comprehensive understanding of the relationship between OP and emission sources, with a particular focus on short-term atmospheric processes that traditional sampling strategies are unable to resolve.

https://doi.org/10.5194/egusphere-2026-4293
Preprint. Discussion started: 30 July 2026

This study represents the initial evaluation of the instrument, establishing its sensitivity, stability, and response to key processes under controlled conditions. This rigorous, stepwise validation is a necessary prerequisite before its deployment in complex ambient environments, which is the focus of our ongoing research. While the instrument has not yet been validated for routine field deployment, these results highlight the potential of high time resolution OP measurements to provide new opportunities to better characterize exposure, and to improve and refine mitigation strategies aimed at reducing PM-related health impacts.

Future work will focus on deploying this instrument in ambient environments to further investigate the influence of SOA and transient reactive species on OP. In parallel, more work is required to align the emerging online OP measurement approaches, with the objective of facilitating cross-study comparability and supporting the development of standardized protocols. A direct intercomparison with established offline DTT methods will also be conducted as part of future field studies, in order to benchmark the system while further assessing the added value of high-time-resolution online measurements.

Code and data availability

Data will be made available on request.

Supplement link

The link to the supplement will be included by Copernicus, if applicable.

Author contributions

T.A designed and developed the measurement and data acquisition system, performed the tests, participated in the simulation chamber experiments, processed the data, created the visualizations and wrote the original draft and reviewed the manuscript. A.D conducted the simulation chamber experiments, contributed to data collection and processing and reviewed the manuscript. M.G contributed to instrument development. J.B.L developed the measurement and data acquisition system. M.C is a principal investigator of the simulation chamber, participated in the simulation chamber experiments and contributed to data collection. E.Pa participated in the simulation chamber experiments and contributed to data collection. B.P.V. is a principal investigator of the simulation chamber and reviewed the manuscript. P.C participated in the simulation chamber experiments, provided funding and reviewed the manuscript. E.Pe and L.Y.A contributed to instrument development, provided funding, participated in discussions on data interpretation and reviewed the manuscript. D.R contributed to instrument development, participated in the simulation chamber experiments, participated in discussions on data interpretation, provided funding, reviewed the manuscript, and supervised the project. All authors read and approved the final manuscript.

https://doi.org/10.5194/egusphere-2026-4293
Preprint. Discussion started: 30 July 2026

Competing interests

The authors declare that they have no known competing financial interests or personal relationships that could have appeared to influence the work reported in this paper.

Disclaimer

Copernicus Publications remains neutral with regard to jurisdictional claims made in the text, published maps, institutional affiliations, or any other geographical representation in this paper. While Copernicus Publications makes every effort to include appropriate place names, the final responsibility lies with the authors. Views expressed in the text are those of the authors and do not necessarily reflect the views of the publisher.

Acknowledgements

This work was carried out as part of the METRONOME project funded by the PNREST Anses, ANSES-23-EST-163. IMT Nord Europe would like to thank the Hauts-de-France Region, the Ministry of Education and Research and the European Regional Economic Development Fund for their financial support for the CPER ECRIN project and acknowledges financial support from the CARINGS program of Carnot M.I.N.E.S, the Labex CaPPA project (ANR-11-LABX-0005-01), which is funded by the French National Research Agency (ANR) through the PIA (Programme d'Investissement d'Avenir), and the CDP AREA (R-CDP-24-003-AREA). The authors acknowledge CNRS-INSU for supporting CESAM platform as a component of the ACTRIS Research Infrastructure.

References

Abrams, J. Y., Weber, R. J., Klein, M., Samat, S. E., Chang, H. H., Strickland, M. J., Verma, V., Fang, T., Bates, J. T., Mulholland, J. A., Russell, A. G., and Tolbert, P. E.: Associations between Ambient Fine Particulate Oxidative Potential and Cardiorespiratory Emergency Department Visits, Environmental Health Perspectives, 125, 107008, https://doi.org/10.1289/EHP1545, 2017.

Badali, K. M., Zhou, S., Aljawhary, D., Antiñolo, M., Chen, W. J., Lok, A., Mungall, E., Wong, J. P. S., Zhao, R., and Abbatt, J. P. D.: Formation of hydroxyl radicals from photolysis of secondary organic aerosol material, Atmospheric Chemistry and Physics, 15, 7831–7840, https://doi.org/10.5194/acp-15-7831-2015, 2015.

Barbero, A., Freche, G., Piard, L., Richard, L., Mhadhbi, T., Marsal, A., Houdier, S., Camman, J., Brezins, M., Golly, B., Jaffrezo, J.-L., and Uzu, G.: Qualification of an online device for the measurement of the oxidative potential of atmospheric particulate matter, Atmospheric Measurement Techniques, 18, 7085–7104, https://doi.org/10.5194/amt-18-7085-2025, 2025.

https://doi.org/10.5194/egusphere-2026-4293
Preprint. Discussion started: 30 July 2026

Basnet, S., Hartikainen, A., Virkkula, A., Yli-Pirilä, P., Kortelainen, M., Suhonen, H., Kilpeläinen, L., Ihalainen, M., Väätäinen, S., Louhisalmi, J., Somero, M., Tissari, J., Jakobi, G., Zimmermann, R., Kilpeläinen, A., and Sippula, O.: Contribution of brown carbon to light absorption in emissions of European residential biomass combustion appliances, Atmospheric Chemistry and Physics, 24, 3197–3215, https://doi.org/10.5194/acp-24-3197-2024, 2024.

Bates, J. T., Weber, R. J., Abrams, J., Verma, V., Fang, T., Klein, M., Strickland, M. J., Sarnat, S. E., Chang, H. H., Mulholland, J. A., Tolbert, P. E., and Russell, A. G.: Reactive Oxygen Species Generation Linked to Sources of Atmospheric Particulate Matter and Cardiorespiratory Effects, Environ. Sci. Technol., 49, 13605–13612, https://doi.org/10.1021/acs.est.5b02967, 2015.

Bates, J. T., Fang, T., Verma, V., Zeng, L., Weber, R. J., Tolbert, P. E., Abrams, J. Y., Sarnat, S. E., Klein, M., Mulholland, J. A., and Russell, A. G.: Review of Acellular Assays of Ambient Particulate Matter Oxidative Potential: Methods and Relationships with Composition, Sources, and Health Effects, Environ. Sci. Technol., 53, 4003–4019, https://doi.org/10.1021/acs.est.8b03430, 2019.

Birmili, W., Allen, A. G., Bary, F., and Harrison, R. M.: Trace Metal Concentrations and Water Solubility in Size-Fractionated Atmospheric Particles and Influence of Road Traffic, Environ. Sci. Technol., 40, 1144–1153, https://doi.org/10.1021/es0486925, 2006.

Borlaza, L. J., Weber, S., Marsal, A., Uzu, G., Jacob, V., Besombes, J.-L., Chatain, M., Conil, S., and Jaffrezo, J.-L.: Nine-year trends of PM_{10} sources and oxidative potential in a rural background site in France, Atmospheric Chemistry and Physics, 22, 8701–8723, https://doi.org/10.5194/acp-22-8701-2022, 2022.

Bressi, M., Cavalli, F., Belis, C. A., Putaud, J.-P., Fröhlich, R., Martins Dos Santos, S., Petralia, E., Prévôt, A. S. H., Berico, M., Malaguti, A., and Canonaco, F.: Variations in the chemical composition of the submicron aerosol and in thesources of the organic fraction at a regional background site of the Po Valley (Italy), Atmos. Chem. Phys., 16, 12875–12896, https://doi.org/10.5194/acp-16-12875-2016, 2016.

Calas, A., Uzu, G., Kelly, F. J., Houdier, S., Martins, J. M. F., Thomas, F., Molton, F., Charron, A., Dunster, C., Oliete, A., Jacob, V., Besombes, J.-L., Chevrier, F., and Jaffrezo, J.-L.: Comparison between five acellular oxidative potential measurement assays performed with detailed chemistry on PM_{10} samples from the city of Chamonix (France), Atmospheric Chemistry and Physics, 18, 7863–7875, https://doi.org/10.5194/acp-18-7863-2018, 2018.

Campbell, S. J., Utinger, B., Barth, A., Paulson, S. E., and Kalberer, M.: Iron and Copper Alter the Oxidative Potential of Secondary Organic Aerosol: Insights from Online Measurements and Model Development, Environ. Sci. Technol., 57, 13546–13558, https://doi.org/10.1021/acs.est.3c01975, 2023.

Campbell, S. J., Barth, A., Chen, G. I., Tremper, A. H., Priestman, M., Ek, D., Gu, S., Kelly, F. J., Kalberer, M., and Green, D. C.: High time resolution quantification of PM2.5 oxidative potential at a Central London roadside supersite, Environment International, 193, 109102, https://doi.org/10.1016/j.envint.2024.109102, 2024.

Campbell, S. J., Utinger, B., Barth, A., Leni, Z., Zhang, Z.-H., Resch, J., Li, K., Steimer, S. S., Banach, C., Gfeller, B., Wragg, F. P. H., Westwood, J., Wolfer, K., Bukowiecki, N., Ihalainen, M., Yli-Pirilä, P., Somero, M., Kortelainen, M., Louhisalmi,

https://doi.org/10.5194/egusphere-2026-4293
Preprint. Discussion started: 30 July 2026

J., Sklorz, M., Czech, H., di Bucchianico, S., Streibel, T., Delaval, M. N., Ruger, C., Baumlin, N., Salathe, M., Fang, Z., Pardo, M., D'Aronco, S., Giorio, C., Shi, Z., Harrison, R. M., Green, D. C., Kelly, F. J., Rudich, Y., Paulson, S. E., Sippula, O., Zimmermann, R., Geiser, M., and Kalberer, M.: Short-lived reactive components substantially contribute to particulate matter oxidative potential, Science Advances, 11, eadp8100, https://doi.org/10.1126/sciadv.adp8100, 2025.

Charrier, J. G. and Anastasio, C.: On dithiothreitol (DTT) as a measure of oxidative potential for ambient particles: evidence for the importance of soluble transition metals, Atmospheric Chemistry and Physics, 12, 9321–9333, https://doi.org/10.5194/acp-12-9321-2012, 2012.

Charrier, J. G., Richards-Henderson, N. K., Bein, K. J., McFall, A. S., Wexler, A. S., and Anastasio, C.: Oxidant production from source-oriented particulate matter – Part 1: Oxidative potential using the dithiothreitol (DTT) assay, Atmospheric Chemistry and Physics, 15, 2327–2340, https://doi.org/10.5194/acp-15-2327-2015, 2015.

Charrier, J. G., McFall, A. S., Vu, K. K.-T., Baroi, J., Olea, C., Hasson, A., and Anastasio, C.: A bias in the "mass-normalized" DTT response – An effect of non-linear concentration-response curves for copper and manganese, Atmospheric Environment, 144, 325–334, https://doi.org/10.1016/j.atmosenv.2016.08.071, 2016.

Chen, H. and Yu, J. Z.: An online instrument for assessing oxidative potential of ambient particulate matter via dithiothreitol assay, using particle-into-liquid sampler (PILS) coupled with improved light absorption measurement, Atmospheric Environment, 343, 120980, https://doi.org/10.1016/j.atmosenv.2024.120980, 2025.

Cheung, R. K. Y., Qi, L., Manousakas, M. I., Puthussery, J. V., Zheng, Y., Koenig, T. K., Cui, T., Wang, T., Ge, Y., Wei, G., Kuang, Y., Sheng, M., Cheng, Z., Li, A., Li, Z., Ran, W., Xu, W., Zhang, R., Han, Y., Wang, Q., Wang, Z., Sun, Y., Cao, J., Slowik, J. G., Dällenbach, K. R., Verma, V., Gysel-Beer, M., Qiu, X., Chen, Q., Shang, J., El-Haddad, I., Prévôt, A. S. H., and Modini, R. L.: Major source categories of PM2.5 oxidative potential in wintertime Beijing and surroundings based on online dithiothreitol-based field measurements, Science of The Total Environment, 928, 172345, https://doi.org/10.1016/j.scitotenv.2024.172345, 2024.

Cho, A. K., Sioutas, C., Miguel, A. H., Kumagai, Y., Schmitz, D. A., Singh, M., Eiguren-Fernandez, A., and Froines, J. R.: Redox activity of airborne particulate matter at different sites in the Los Angeles Basin, Environmental Research, 99, 40–47, https://doi.org/10.1016/j.envres.2005.01.003, 2005.

Delfino, R. J., Staimer, N., Tjoa, T., Gillen, D. L., Schauer, J. J., and Shafer, M. M.: Airway inflammation and oxidative potential of air pollutant particles in a pediatric asthma panel, J Expo Sci Environ Epidemiol, 23, 466–473, https://doi.org/10.1038/jes.2013.25, 2013.

Dellinger, B., Pryor, W. A., Cueto, R., Squadrito, G. L., Hegde, V., and Deutsch, W. A.: Role of Free Radicals in the Toxicity of Airborne Fine Particulate Matter, Chem. Res. Toxicol., 14, 1371–1377, https://doi.org/10.1021/tx010050x, 2001.

Dominutti, P. A., Jaffrezo, J.-L., Marsal, A., Mhadhbi, T., Elazzouzi, R., Rak, C., Cavalli, F., Putaud, J.-P., Bougiatioti, A., Mihalopoulos, N., Paraskevopoulou, D., Mudway, I., Nenes, A., Daellenbach, K. R., Banach, C., Campbell, S. J., Cigánková, H., Contini, D., Evans, G., Georgopoulou, M., Ghanem, M., Glencross, D. A., Guascito, M. R., Herrmann, H., Iram, S., Jovanović, M., Jovašević-Stojanović, M., Kalberer, M., Kooter, I. M., Paulson, S. E., Patel, A., Perdrix, E., Pietrogrande, M.

https://doi.org/10.5194/egusphere-2026-4293
Preprint. Discussion started: 30 July 2026

C., Mikuška, P., Sauvain, J.-J., Seitanidi, K., Shahpoury, P., Souza, E. J. d S., Steimer, S., Stevanovic, S., Suarez, G., Subramanian, P. S. G., Utinger, B., van Os, M. F., Verma, V., Wang, X., Weber, R. J., Yang, Y., Querol, X., Hoek, G., Harrison, R. M., and Uzu, G.: An interlaboratory comparison to quantify oxidative potential measurement in aerosol particles: challenges and recommendations for harmonisation, Atmospheric Measurement Techniques, 18, 177–195, https://doi.org/10.5194/amt-18-177-2025, 2025.

Eiguren Fernandez, A., Lewis, G. S., and Hering, S. V.: Design and Laboratory Evaluation of a Sequential Spot Sampler for Time-Resolved Measurement of Airborne Particle Composition, Aerosol Science and Technology, 48, 655–663, https://doi.org/10.1080/02786826.2014.911409, 2014.

Eiguren-Fernandez, A., Kreisberg, N., and Hering, S.: An online monitor of the oxidative capacity of aerosols (o-MOCA), Atmos. Meas. Tech., 10, 633–644, https://doi.org/10.5194/amt-10-633-2017, 2017.

European Parliament: Directive (EU) 2024/2881 of the European Parliament and of the Council of 23 October 2024 on ambient air quality and cleaner air for Europe, 2024.

Fuchs, H., Illmann, N., Muñoz, A., Ródenas, M., Picquet-Varrault, B., Alfarra, M. R., Arsene, C., Bejan, I. G., Bell, D. M., Bilde, M., Böhmländer, A., Campos-Pineda, M., Cazaunau, M., Coll, P., Daële, V., Di Biagio, C., Flynn, M., Formenti, P., Herrmann, H., Höhler, K., Hohaus, T., Johnson, M. S., Juurola, E., Kivekäs, N., Kaiser, J., Kaltsonoudis, C., Laj, P., Massabò, D., Mazzei, F., McFiggans, G., McGillen, M. R., Mellouki, A., Mettke, P., Möhler, O., Mothes, F., Niedermeier, D., Novelli, A., Olariu, R. I., Pandis, S. N., Patroescu-Klotz, I., Petracca Altieri, R. M., Prati, P., Roman, C., Ruth, A. A., Saathoff, H., Schmalfuß, S., Stratmann, F., Vernocchi, V., Voliotis, A., Voigtländer, J., Virtanen, A., Wahner, A., Wagner, R., Wenger, J., Zorn, S., Wiesen, P., and Doussin, J.-F.: Atmospheric Simulation Chambers in the ACTRIS Research Infrastructure, EGUsphere, 1–53, https://doi.org/10.5194/egusphere-2026-1612, 2026.

Fuller, S. J., Wragg, F. P. H., Nutter, J., and Kalberer, M.: Comparison of on-line and off-line methods to quantify reactive oxygen species (ROS) in atmospheric aerosols, Atmospheric Environment, 92, 97–103, https://doi.org/10.1016/j.atmosenv.2014.04.006, 2014.

Gauderman, J. W., McConnell, R., Gilliland, F., London, S., Thomas, D., Avol, E., Vora, H., Berhane, K., Rappaport, E. B., Lurmann, F., Margolis, H. G., and Peters, J.: Association between Air Pollution and Lung Function Growth in Southern California Children, Am J Respir Crit Care Med, 162, 1383–1390, https://doi.org/10.1164/ajrccm.162.4.9909096, 2000.

Georgopoulou, M. P., Macias Rodriguez, J. C., Yegen, C.-H., Kaltsonoudis, C., Cazaunau, M., Vasilakopoulou, C. N., Matrali, A., Seitanidi, K., Aktypis, A., Nenes, A., Buissot, C., Gratien, A., Berge, A., Pangui, E., Al Marj, E., Gerard, L., Varrault, B. P., Lanone, S., Coll, P., and Pandis, S. N.: A coupled atmospheric simulation chamber system for the production of realistic aerosols and preclinical model exposure, Air Qual Atmos Health, 17, 2909–2930, https://doi.org/10.1007/s11869-024-01611-5, 2024.

Ghanem, M., Perdrix, E., Alleman, L. Y., Rousset, D., and Coddeville, P.: Phosphate Buffer Solubility and Oxidative Potential of Single Metals or Multielement Particles of Welding Fumes, Atmosphere, 12, 30, https://doi.org/10.3390/atmos12010030, 2021.

https://doi.org/10.5194/egusphere-2026-4293
Preprint. Discussion started: 30 July 2026

Ghanem, M., Alleman, L. Y., Rousset, D., Perdrix, E., and Coddeville, P.: Experimental factors influencing the bioaccessibility and the oxidative potential of transition metals from welding fumes, Environ. Sci.: Processes Impacts, 26, 843–857, https://doi.org/10.1039/D3EM00546A, 2024.

Ghazaly, C.: Développement d'un capteur spectrophotométrique pour la mesure en temps réel des expositions professionnelles à l'ozone, PhD Thesis, Université de Lorraine, 187 pp., 2019.

Haase, L.-M., Birk, T., Bachand, A. M., and Mundt, K. A.: A Health Surveillance Study of Workers Employed at a Copper Smelter-Effects of Long-Term Exposure to Copper on Lung Function Using Spirometric Data, J Occup Environ Med, 63, e480–e489, https://doi.org/10.1097/JOM.0000000000002252, 2021.

Harrison, R. M. and Yin, J.: Particulate matter in the atmosphere: which particle properties are important for its effects on health?, Science of The Total Environment, 249, 85–101, https://doi.org/10.1016/S0048-9697(99)00513-6, 2000.

He, L. and Zhang, J.: Particulate matter (PM) oxidative potential: Measurement methods and links to PM physicochemical characteristics and health effects, Critical Reviews in Environmental Science and Technology, 53, 177–197, https://doi.org/10.1080/10643389.2022.2050148, 2023.

Hellack, B., Nickel, C., Albrecht, C., Kuhlbusch, T. A. J., Boland, S., Baeza-Squiban, A., Wohlleben, W., and Schins, R. P. F.: Analytical methods to assess the oxidative potential of nanoparticles: a review, Environ. Sci.: Nano, 4, 1920–1934, https://doi.org/10.1039/C7EN00346C, 2017.

Huang, R.-J., Zhang, Y., Bozzetti, C., Ho, K.-F., Cao, J.-J., Han, Y., Daellenbach, K. R., Slowik, J. G., Platt, S. M., Canonaco, F., Zotter, P., Wolf, R., Pieber, S. M., Bruns, E. A., Crippa, M., Ciarelli, G., Piazzalunga, A., Schwikowski, M., Abbaszade, G., Schnelle-Kreis, J., Zimmermann, R., An, Z., Szidat, S., Baltensperger, U., Haddad, I. E., and Prévôt, A. S. H.: High secondary aerosol contribution to particulate pollution during haze events in China, Nature, 514, 218–222, https://doi.org/10.1038/nature13774, 2014.

Janssen, N. A. H., Strak, M., Yang, A., Hellack, B., Kelly, F. J., Kuhlbusch, T. A. J., Harrison, R. M., Brunekreef, B., Cassee, F. R., Steenhof, M., and Hoek, G.: Associations between three specific a-cellular measures of the oxidative potential of particulate matter and markers of acute airway and nasal inflammation in healthy volunteers, Occup Environ Med, 72, 49–56, https://doi.org/10.1136/oemed-2014-102303, 2015.

Jiang, H. and Jang, M.: Dynamic Oxidative Potential of Atmospheric Organic Aerosol under Ambient Sunlight, Environ. Sci. Technol., 52, 7496–7504, https://doi.org/10.1021/acs.est.8b00148, 2018.

Kachur, A. V., Held, K. D., Koch, C. J., and Biaglow, J. E.: Mechanism of Production of Hydroxyl Radicals in the Copper-Catalyzed Oxidation of Dithiothreitol, Radiation Research, 147, 409–415, https://doi.org/10.2307/3579496, 1997.

Kelly, F. J.: Oxidative stress: its role in air pollution and adverse health effects, Occupational and Environmental Medicine, 60, 612–616, https://doi.org/10.1136/oem.60.8.612, 2003.

Kelly, F. J. and Fussell, J. C.: Size, source and chemical composition as determinants of toxicity attributable to ambient particulate matter, Atmospheric Environment, 60, 504–526, https://doi.org/10.1016/j.atmosenv.2012.06.039, 2012.

https://doi.org/10.5194/egusphere-2026-4293
Preprint. Discussion started: 30 July 2026

Khlystov, A., Wyers, G. P., and Slanina, J.: The steam-jet aerosol collector, Atmospheric Environment, 29, 2229–2234, https://doi.org/10.1016/1352-2310(95)00180-7, 1995.

King, L. E. and Weber, R. J.: Development and testing of an online method to measure ambient fine particulate reactive oxygen species (ROS) based on the 2',7'-dichlorofluorescin (DCFH) assay, Atmospheric Measurement Techniques, 6, 1647–1658, https://doi.org/10.5194/amt-6-1647-2013, 2013.

Knaapen, A. M., Borm, P. J. A., Albrecht, C., and Schins, R. P. F.: Inhaled particles and lung cancer. Part A: Mechanisms, International Journal of Cancer, 109, 799–809, https://doi.org/10.1002/ijc.11708, 2004.

Koehler, K. A., Shapiro, J., Sameenoi, Y., Henry, C., and Volckens, J.: Laboratory Evaluation of a Microfluidic Electrochemical Sensor for Aerosol Oxidative Load, Aerosol Science and Technology, 48, 489–497, https://doi.org/10.1080/02786826.2014.891722, 2014.

Kumagai, Y., Koide, S., Taguchi, K., Endo, A., Nakai, Y., Yoshikawa, T., and Shimojo, N.: Oxidation of Proximal Protein Sulfhydryls by Phenanthraquinone, a Component of Diesel Exhaust Particles, Chem. Res. Toxicol., 15, 483–489, https://doi.org/10.1021/tx0100993, 2002.

Lakey, P. S. J., Berkemeier, T., Tong, H., Arangio, A. M., Lucas, K., Pöschl, U., and Shiraiwa, M.: Chemical exposure-response relationship between air pollutants and reactive oxygen species in the human respiratory tract, Sci Rep, 6, 32916, https://doi.org/10.1038/srep32916, 2016.

Lelieveld, J., Evans, J. S., Fnais, M., Giannadaki, D., and Pozzer, A.: The contribution of outdoor air pollution sources to premature mortality on a global scale, Nature, 525, 367–371, https://doi.org/10.1038/nature15371, 2015.

Li, S., Wei, J., Hu, Y., Liu, Y., Hu, M., Shi, Y., Xue, Y., Liu, M., Xie, W., Guo, X., and Liu, X.: Long-term effect of intermediate particulate matter (PM1–2.5) on incident asthma among middle-aged and elderly adults: A national population-based longitudinal study, Science of The Total Environment, 859, 160204, https://doi.org/10.1016/j.scitotenv.2022.160204, 2023.

Lin, M. and Yu, J. Z.: Dithiothreitol (DTT) concentration effect and its implications on the applicability of DTT assay to evaluate the oxidative potential of atmospheric aerosol samples, Environmental Pollution, 251, 938–944, https://doi.org/10.1016/j.envpol.2019.05.074, 2019.

Liu, Q., Sun, Y., Hu, B., Liu, Z., Akio, S., and Wang, Y.: In situ measurement of PM1 organic aerosol in Beijing winter using a high-resolution aerosol mass spectrometer, Chin. Sci. Bull., 57, 819–826, https://doi.org/10.1007/s11434-011-4886-0, 2012.

Liu, X., Zhang, X., Wang, T., Jin, B., Wu, L., Lara, R., Monge, M., Reche, C., Jaffrezo, J.-L., Uzu, G., Dominutti, P., Darfeuil, S., Favez, O., Conil, S., Marchand, N., Castillo, S., de la Rosa, J. D., Stuart, G., Eleftheriadis, K., Diapouli, E., Gini, M. I., Nava, S., Alves, C., Wang, X., Xu, Y., Green, D. C., Beddows, D. C. S., Harrison, R. M., Alastuey, A., and Querol, X.: PM10-bound trace elements in pan-European urban atmosphere, Environmental Research, 260, 119630, https://doi.org/10.1016/j.envres.2024.119630, 2024.

https://doi.org/10.5194/egusphere-2026-4293
Preprint. Discussion started: 30 July 2026

Manfrin, A., Nizkorodov, S. A., Malecha, K. T., Getzinger, G. J., McNeill, K., and Borduas-Dedekind, N.: Reactive Oxygen Species Production from Secondary Organic Aerosols: The Importance of Singlet Oxygen, Environ. Sci. Technol., 53, 8553–8562, https://doi.org/10.1021/acs.est.9b01609, 2019.

Miller, J. C. and Miller, J. N.: Statistics for analytical chemistry, New York : Ellis Horwood PTR Prentice Hall, 246 pp., 1993.

Mishra, A., Lelieveld, S., Krüger, M., Campbell, S. J., Srivastava, D., Lanzafame, G. M., Tomaz, S., Favez, O., Bonnaire, N., Lucarelli, F., Alleman, L. Y., Uzu, G., Jaffrezo, J.-L., Chen, G. I., Green, D. C., Priestman, M., Tremper, A. H., Barth, A., Kalberer, M., Bandowe, B. A. M., Lammel, G., Pöschl, U., Shahpoury, P., Albinet, A., and Berkemeier, T.: Aerosol oxidative potential and reactive species predicted with a chemical kinetics model (KM-OP), EGUsphere, 1–39, https://doi.org/10.5194/egusphere-2026-566, 2026.

Nel, A., Xia, T., Mädler, L., and Li, N.: Toxic Potential of Materials at the Nanolevel, Science, 311, 622–627, https://doi.org/10.1126/science.1114397, 2006.

Orsini, D., Ma, Y., Sullivan, A., Sierau, B., Baumann, K., and Weber, R. J.: Refinements to the particle-into-liquid sampler (PILS) for ground and airborne measurements of water soluble aerosol composition, Atmospheric Environment, 37, 1243–1259, https://doi.org/10.1016/S1352-2310(02)01015-4, 2003.

Pant, P. and Harrison, R. M.: Estimation of the contribution of road traffic emissions to particulate matter concentrations from field measurements: A review, Atmospheric Environment, 77, 78–97, https://doi.org/10.1016/j.atmosenv.2013.04.028, 2013.

Pietrogrande, M. C., Bacco, D., Demaria, G., Russo, M., Scotto, F., and Trentini, A.: Polycyclic aromatic hydrocarbons and their oxygenated derivatives in urban aerosol: levels, chemical profiles, and contribution to PM2.5 oxidative potential, Environ Sci Pollut Res Int, 29, 54391–54406, https://doi.org/10.1007/s11356-021-16858-z, 2022.

Poulakis, E., Theodosi, C., Bressi, M., Sciare, J., Ghersi, V., and Mihalopoulos, N.: Airborne mineral components and trace metals in Paris region: spatial and temporal variability, Environ Sci Pollut Res, 22, 14663–14672, https://doi.org/10.1007/s11356-015-4679-0, 2015.

Puthussery, J. V., Zhang, C., and Verma, V.: Development and field testing of an online instrument for measuring the real-time oxidative potential of ambient particulate matter based on dithiothreitol assay, Atmos. Meas. Tech., 11, 5767–5780, https://doi.org/10.5194/amt-11-5767-2018, 2018.

Queron, J., De Mendonça Andrade, M., Le Bihan, O., Lacroix, G., Uzu, G., Suarez, G., Ngo, S., Delater, A., Fable, S., Meunier, L., Tebby, C., Amara, A., Bonnaire, N., Petit, J.-E., Benbekka, R., Gros, V., and Durif, M.: Caractérisations toxicologiques in vitro, chimiques et physiques de particules prélevées dans l'air d'habitacles de transport en roulage, ADEME, 2022.

Ringuet, J., Leoz-Garziandia, E., Budzinski, H., Villenave, E., and Albinet, A.: Particle size distribution of nitrated and oxygenated polycyclic aromatic hydrocarbons (NPAHs and OPAHs) on traffic and suburban sites of a European megacity: Paris (France), Atmospheric Chemistry and Physics, 12, 8877–8887, https://doi.org/10.5194/acp-12-8877-2012, 2012.

Sameenoi, Y., Koehler, K., Shapiro, J., Boonsong, K., Sun, Y., Collett, J., Volckens, J., and Henry, C. S.: Microfluidic Electrochemical Sensor for On-Line Monitoring of Aerosol Oxidative Activity, J. Am. Chem. Soc., 134, 10562–10568, https://doi.org/10.1021/ja3031104, 2012.

https://doi.org/10.5194/egusphere-2026-4293
Preprint. Discussion started: 30 July 2026

Shahpoury, P., Zhang, Z. W., Filippi, A., Hildmann, S., Lelieveld, S., Mashtakov, B., Patel, B. R., Traub, A., Umbrio, D., Wietzoreck, M., Wilson, J., Berkemeier, T., Celo, V., Dabek-Zlotorzynska, E., Evans, G., Harner, T., Kerman, K., Lammel, G., Noroozifar, M., Pöschl, U., and Tong, H.: Inter-comparison of oxidative potential metrics for airborne particles identifies differences between acellular chemical assays, Atmospheric Pollution Research, 13, 101596, https://doi.org/10.1016/j.apr.2022.101596, 2022.

Strak, M., Janssen, N., Beelen, R., Schmitz, O., Vaartjes, I., Karssenberg, D., van den Brink, C., Bots, M. L., Dijst, M., Brunekreef, B., and Hoek, G.: Long-term exposure to particulate matter, NO2 and the oxidative potential of particulates and diabetes prevalence in a large national health survey, Environment International, 108, 228–236, https://doi.org/10.1016/j.envint.2017.08.017, 2017.

Tassel, C., Jaffrezo, J.-L., Dominutti, P., Daellenbach, K. R., Darfeuil, S., Elazzouzi, R., Laj, P., Marsal, A., Mhadhbi, T., Dinh, V. N. T., Voiron, C., Houdier, S., Durif, M., Chatain, M., Francony, F., Cozic, J., Salque Moreton, G., Le Quilleuc, M., Ghersi, V., Gille, G., Mesbah, B., Stratigou, E., Zublena, M., Diémoz, H., Alastuey, A., D'Anna, B., Marchand, N., Conil, S., Gros, V., van Os, M. F., Salma, I., Mihalopoulos, N., Močnik, G., Džepina, K., Styszko, K., Hüglin, C., Querol, X., Prévôt, A. S. H., Favez, O., Siroux, V., and Uzu, G.: Oxidative potential of atmospheric particles in Europe and exposure scenarios, Nature, 1–6, https://doi.org/10.1038/s41586-025-09666-9, 2025.

Tuet, W. Y., Chen, Y., Xu, L., Fok, S., Gao, D., Weber, R. J., and Ng, N. L.: Chemical oxidative potential of secondary organic aerosol (SOA) generated from the photooxidation of biogenic and anthropogenic volatile organic compounds, Atmospheric Chemistry and Physics, 17, 839–853, https://doi.org/10.5194/acp-17-839-2017, 2017.

Utinger, B., Campbell, S. J., Bukowiecki, N., Barth, A., Gfeller, B., Freshwater, R., Rüegg, H.-R., and Kalberer, M.: An automated online field instrument to quantify the oxidative potential of aerosol particles via ascorbic acid oxidation, Atmospheric Measurement Techniques, 16, 2641–2654, https://doi.org/10.5194/amt-16-2641-2023, 2023.

Wang, J., Doussin, J. F., Perrier, S., Perraudin, E., Katrib, Y., Pangui, E., and Picquet-Varrault, B.: Design of a new multi-phase experimental simulation chamber for atmospheric photosmog, aerosol and cloud chemistry research, Atmospheric Measurement Techniques, 4, 2465–2494, https://doi.org/10.5194/amt-4-2465-2011, 2011a.

Wang, Y., Hopke, P. K., Sun, L., Chalupa, D. C., and Utell, M. J.: Laboratory and Field Testing of an Automated Atmospheric Particle-Bound Reactive Oxygen Species Sampling-Analysis System, Journal of Toxicology, 2011, 419476, https://doi.org/10.1155/2011/419476, 2011b.

Wragg, F. P. H., Fuller, S. J., Freshwater, R., Green, D. C., Kelly, F. J., and Kalberer, M.: An automated online instrument to quantify aerosol-bound reactive oxygen species (ROS) for ambient measurement and health-relevant aerosol studies, Atmospheric Measurement Techniques, 9, 4891–4900, https://doi.org/10.5194/amt-9-4891-2016, 2016.

Wu, J., Yang, C., Zhang, C., Cao, F., Wu, A., and Zhang, Y.: Development, characterization, and application of an improved online reactive oxygen species analyzer based on the Monitor for AeRosols and Gases in ambient Air (MARGA), Atmospheric Measurement Techniques, 15, 2623–2633, https://doi.org/10.5194/amt-15-2623-2022, 2022.

https://doi.org/10.5194/egusphere-2026-4293
Preprint. Discussion started: 30 July 2026

Yang, A., Janssen, N. A. H., Brunekreef, B., Cassee, F. R., Hoek, G., and Gehring, U.: Children's respiratory health and oxidative potential of PM2.5: the PIAMA birth cohort study, Occup Environ Med, 73, 154–160, https://doi.org/10.1136/oemed-2015-103175, 2016.

Yang, M., Wu, Q.-Z., Zhang, Y.-T., Leskinen, A., Komppula, M., Hakkarainen, H., Roponen, M., Xu, S.-L., Lin, L.-Z., Liu, R.-Q., Hu, L.-W., Yang, B.-Y., Zeng, X.-W., Dong, G.-H., and Jalava, P.: Concentration, chemical composition and toxicological responses of the ultrafine fraction of urban air particles in PM1, Environment International, 170, 107661, https://doi.org/10.1016/j.envint.2022.107661, 2022.

Yang, T., Wang, J., Huang, J., Kelly, F. J., and Li, G.: Long-term Exposure to Multiple Ambient Air Pollutants and Association With Incident Depression and Anxiety, JAMA Psychiatry, https://doi.org/10.1001/jamapsychiatry.2022.4812, 2023.